Replica Thermodynamic Trade-off Relations: Entropic Bounds on Network Diffusion and Trajectory Observables

Yoshihiko Hasegawa*
Department of Information and Communication Engineering, Graduate School of Information Science and Technology, The University of Tokyo, Tokyo 113-8656, Japan

(Dated: December 23, 2025)

We introduce replica Markov processes to derive thermodynamic trade-off relations for nonlinear functions of probability distributions. In conventional thermodynamic trade-off relations, the quantities of interest are linear in the underlying probability distribution. Some important information-theoretic quantities, such as Rényi entropies, are nonlinear; however, such nonlinearities are generally more difficult to handle. Inspired by replica techniques used in quantum information and spin-glass theory, we construct Markovian dynamics of identical replicas and derive a lower bound on relative moments in terms of the dynamical activity. We apply our general result to two scenarios. First, for a random walker on a network, we derive an upper bound on the Rényi entropy of the position distribution of the walker, which quantifies the extent of diffusion on the network. Remarkably, the bound is expressed solely in terms of escape rate from the initial node, and thus depends only on local information. Second, we consider trajectory observables in Markov processes and obtain an upper bound on the Rényi entropy of the distribution of these observables, again in terms of the dynamical activity. This provides an entropic characterization of uncertainty that generalizes existing variance-based thermodynamic uncertainty relations.

INTRODUCTION

In quantum information and statistical mechanics, one often needs to compute expectation values of nonlinear physical quantities. For example, purity requires the square of the density operator, $\mathrm{Tr}[\rho^2]$. Although purity serves as a key quantity for distinguishing quantum from classical behavior, its experimental measurement is known to be difficult. The swap trick [1] is a technique to measure purity without performing state tomography. The swap trick uses the following identity:

$$\mathrm{Tr}[\rho^2] = \mathrm{Tr}[(\rho \otimes \rho)\,\mathrm{SWAP}], \tag{1}$$

where SWAP denotes the swap operator. The identity given in Eq. (1) shows that the purity $\mathrm{Tr}[\rho^2]$ can be obtained by preparing two replicas of ρ and measuring the expectation value of the SWAP operator acting on $\rho \otimes \rho$. This avoids full state tomography of ρ, which would require many measurement shots to reliably estimate ρ^2. The use of replicas has been highly effective in classical shadow tomography [2–4] or in the study of the barren plateau in parametrized quantum circuits [5]. The application of *hypothetical* replicas to the evaluation of nonlinear quantities has a long-standing history. In spin glasses [6–8], for example, we often need to evaluate the disorder average of the logarithm of the partition function $\mathbb{E}[\ln Z]$, which is difficult to compute directly. The replica method addresses this by introducing n replicas of the system and expressing the logarithm as a limit $\ln Z = \lim_{n\to 0}(Z^n - 1)/n$. This technique has been widely used in the analysis of learning theory [9–13] and conformal field theory [14, 15] . These examples illustrate the power of using replicas to calculate expectations of nonlinear quantities.

In this paper, we consider a Markov process consisting of identical replica processes in the context of thermodynamic trade-off relations. Over the past decade, thermodynamic trade-off relations have been extensively studied in stochastic and quantum thermodynamics. In the thermodynamic uncertainty relations [16–36], trajectory observables are considered and lower bounds on their relative variance are derived, where the bounds involve the entropy production and the dynamical activity. Extensions of these uncertainty relations to the quantum domain have been actively studied [32, 33, 36–39]. Related work has also examined how to compute state-dependent expectation values [40, 41]. What these relations have in common is that the quantities being computed are linear in the underlying probabilities. For example, in thermodynamic uncertainty relations, we are often interested in quantities of the form

$$\mathbb{E}[f] = \sum_{\Gamma} \mathcal{P}(\Gamma)\, f(\Gamma), \tag{2}$$

where Γ denotes a stochastic trajectory, $\mathcal{P}(\Gamma)$ is the trajectory probability, and $f(\Gamma)$ is an observable like a current. Equation (2) is linear with respect to probability $\mathcal{P}(\Gamma)$. Typical examples of Eq. (2) include dissipated heat and stochastic displacement. In contrast, nonlinear functions of the probabilities are generally much harder to compute, although they play a crucial role. A prominent example is the Rényi entropy, which measures the degree of uncertainty of a random variable. The thermodynamic uncertainty relation expresses the uncertainty using the variance of an observable. In information theory, however, uncertainty is often quantified using entropy. When

* hasegawa@biom.t.u-tokyo.ac.jp

the output is categorical rather than numerical, the variance is not a natural measure of uncertainty. Entropy, by contrast, applies directly to discrete outcomes and can be used to quantify uncertainty in this setting. For example, when quantifying the extent that a random walker on a network has propagated over the network, variance is not suitable because the states are labels rather than numerical values.

Specifically, we derive a lower bound on relative moments in terms of the dynamical activity [Eq. (12)], which is referred to as *replica trade-off relation*. This relation holds only in the replica process. However, by considering specific scenarios, the replicas become virtual, as in the previously mentioned spin-glass case, and we can derive a trade-off relation that holds in an original single process. Specifically, we consider a random walker on a network whose dynamics obey a continuous-time Markov process. Using the replica trade-off relation, we derive trade-off relations in the Rényi entropy for the probability distribution of the walker position, which quantifies the extent of the diffusion of the walker. The derived bound indicates that the Rényi entropy is bounded from above by the dynamical activity at the initial time, which corresponds to the local escape rate from the initial node and can be computed as the sum of the transition rates from the initial node to all nodes reachable in a single jump. In particular, no matter how large the overall network is, it can be computed using only the local information around the initial node. In the second scenario, we consider trajectory observables in a continuous-time Markov process and consider the probability distribution of the trajectory observables. Using the replica trade-off relation, we obtain the upper bound on the Rényi entropy of the observable distribution, where the upper bound involves the dynamical activity, which quantifies the uncertainty of the observable trajectory. The uncertainty in the trajectory observable has been conventionally studied using the variance, and it was shown that its relative variance is bounded from below by the reciprocal of the dynamical activity. Our result shows that not only the relative variance but also uncertainty based on Rényi entropy is fundamentally constrained by the dynamical activity.

RESULTS

Replica Markov processes

Consider a classical Markov process with D states, represented by $\mathfrak{B} \equiv \{B_1, B_2, \ldots, B_D\}$ (Fig. 1(a)). Let $p_\mu(t)$ be the probability that the system is in state B_μ at time t, and let $W_{\mu'\mu}$ be the transition rate from state B_μ to state $B_{\mu'}$. Here, we assume that the transition rate is time-independent. The time evolution is governed by the master equation:

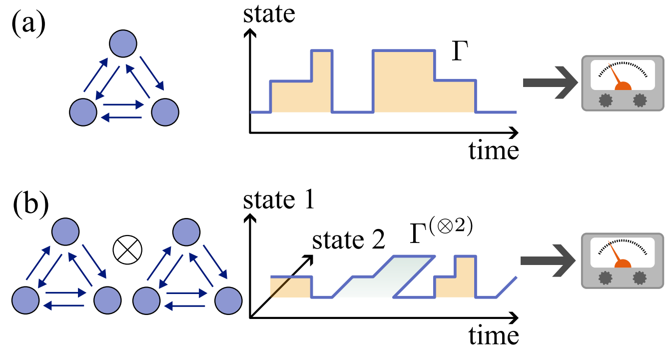

FIG. 1. (a) Single process scenario. This scenario is usually considered in stochastic thermodynamics. Given a Markov process, we consider stochastic trajectories, which are a random realization of the Markov process. We are interested in stochastic quantities associated with trajectories, whose statistics are linear in the trajectory probability. (b) $K = 2$ replica process scenario. We consider two identical Markov processes. The state space is a product space of each Markov process and the trajectories are defined on the product space. We are interested in stochastic quantities of the replica process, which become nonlinear quantities in the original single process.

$$\frac{d}{dt} p_\mu(t) = \sum_{\mu'} W_{\mu\mu'} p_{\mu'}(t), \tag{3}$$

where the diagonal elements are defined by $W_{\mu\mu} = -\sum_{\mu'\neq\mu} W_{\mu'\mu}$. In stochastic thermodynamics, the trajectories generated by the master equation [Eq. (3)] are fundamental for analyzing the system's stochastic dynamics. Several quantities, such as state displacement, dissipated heat, and Shannon entropy, are considered at the level of the stochastic trajectories. We are interested in the dynamics within the time interval $[0, \tau]$ ($\tau > 0$). Suppose that there are J jump events within the interval. Let t_j be the time of the j-th jump and let $X_j \in \mathfrak{B}$ be the state after the j-th jump. The trajectory Γ is then expressed by

$$\Gamma = [(t_0, X_0), (t_1, X_1), \ldots, (t_J, X_J)], \tag{4}$$

where $t_0 = 0$ is the initial time and X_0 is the initial state.

As mentioned in the introduction, we consider replicas of the original process and regard the whole Markov process as a combined process (Fig. 1(b)). For simplicity, here we introduce the case of two replicas. That is, there are two identical processes, where there is *no* interaction between them. It is straightforward to extend this case to scenarios where there are K replica processes. The state space is a product of the two state sets. The set of states in the combined Markov process of two replicas is given by $\mathfrak{B}^{(\otimes 2)} \equiv \{(B_1^{(1)}, B_1^{(2)}), (B_1^{(1)}, B_2^{(2)}), \ldots, (B_D^{(1)}, B_D^{(2)})\}$. Therefore, the number of total states in the combined process is $|\mathfrak{B}^{(\otimes 2)}| = D^2$. From now on, when a superscript (k) is used, it denotes a quantity associated with the k-th process, and when a superscript $(\otimes K)$ is used, it denotes a quantity for the combined system in which all the processes $1, 2, \ldots, K$ are regarded as a single combined process. When we omit the superscript, the corresponding variables refer to those in the single process (i.e., $K = 1$ case).

Let $p_{\mu\nu}^{(\otimes 2)}(t)$ be the probability that the combined system is in state $(B_\mu^{(1)}, B_\nu^{(2)}) \in \mathfrak{B}^{(\otimes 2)}$ at time t. Let $W_{\nu\mu}^{(k)}$ be the transition rate from state $B_\mu^{(k)}$ to state $B_\nu^{(k)}$ in the k-th process. Since we are considering identical processes, $W_{\mu'\mu}^{(k)} = W_{\mu'\mu}$, but we keep the superscript for clarity. The master equation corresponding to the combined process of the two replicas is given by

$$\frac{d}{dt} p_{\mu\nu}^{(\otimes 2)}(t) = \sum_{\mu'} W_{\mu\mu'}^{(1)} p_{\mu'\nu}^{(\otimes 2)}(t) + \sum_{\nu'} W_{\nu\nu'}^{(2)} p_{\mu\nu'}^{(\otimes 2)}(t). \quad (5)$$

As in the case of a single process [Eq. (3)], we can consider a trajectory in the combined process of the two replicas. Suppose that there are J jump events in the trajectory of the combined process within $[0, \tau]$. Let $t_j^{(\otimes 2)}$ be the time of the j-th jump and let $X_j^{(\otimes 2)} \in \mathfrak{B}^{(\otimes 2)}$ be the state after the j-th jump in the combined process. Then, the trajectory is expressed as

$$\Gamma^{(\otimes 2)} = [(t_0^{(\otimes 2)}, X_0^{(\otimes 2)}), (t_1^{(\otimes 2)}, X_1^{(\otimes 2)}), \ldots, (t_J^{(\otimes 2)}, X_J^{(\otimes 2)})], \quad (6)$$

where $t_0 = 0$ and $X_0^{(\otimes 2)}$ is the initial state. For instance, suppose that the trajectories of the first and second processes are

$$\Gamma^{(1)} = [(0, B_1^{(1)}), (1, B_2^{(1)})], \quad (7)$$

$$\Gamma^{(2)} = [(0, B_2^{(2)}), (2, B_3^{(2)}), (3, B_1^{(2)})], \quad (8)$$

The trajectory in the combined process becomes

$$\Gamma^{(\otimes 2)} = \Gamma^{(\otimes 2)}(\Gamma^{(1)}, \Gamma^{(2)}) = [(0, (B_1^{(1)}, B_2^{(2)})), (1, (B_2^{(1)}, B_2^{(2)})), (2, (B_2^{(1)}, B_3^{(2)})), (3, (B_2^{(1)}, B_1^{(2)}))]. \quad (9)$$

where the expression $\Gamma^{(\otimes 2)}(\Gamma^{(1)}, \Gamma^{(2)})$ emphasizes that $\Gamma^{(\otimes 2)}$ can be constructed given $\Gamma^{(1)}$ and $\Gamma^{(2)}$. Here, we have only considered the two-process case. However, it is straightforward to generalize the discussion to more than two processes.

Replica trade-off relations

Introducing the combined process with two replicas, we will focus on general scenario in which there are K replicas. We now introduce observables associated with trajectories. Let $N^{(\otimes K)}(\Gamma^{(\otimes K)})$ be an observable of the trajectory $\Gamma^{(\otimes K)}$, which is the trajectory in the combined process of K replicas. Let $\Gamma_\varnothing^{(\otimes K)}$ be arbitrary trajectory in the combined process in which there is no jump. For example, $\Gamma_\varnothing^{(\otimes K)}$ could be

$$\Gamma_\varnothing^{(\otimes 2)} = \left[(t_0, (B_1^{(1)}, B_1^{(2)}))\right], \quad (10)$$

which consists only of the initial state $(B_1^{(1)}, B_1^{(2)})$. The observable $N^{(\otimes K)}(\Gamma_\varnothing^{(\otimes K)})$ can be arbitrary, provided it satisfies

$$N^{(\otimes K)}(\Gamma_\varnothing^{(\otimes K)}) = 0. \quad (11)$$

A simple example of such an observable in the single process is a counting observable, that count the number of jumps within the time interval $[0, \tau]$. Apparently, such an observable is zero for $\Gamma_\varnothing$ and thus it satisfies the condition of Eq. (11).

Let $\mathbb{E}[X]$ denote the expectation value of a random variable X. Since Γ is a random variable, observable $N^{(\otimes K)}(\Gamma^{(\otimes K)})$ is a random variable as well. We then obtain our first result (see Methods for the derivation):

$$\frac{\mathbb{E}\left[|N^{(\otimes K)}|^s\right]^{r/(s-r)}}{\mathbb{E}\left[|N^{(\otimes K)}|^r\right]^{s/(s-r)}} \geq \frac{1}{1 - e^{-\tau K \mathfrak{a}(t=0)}}, \quad (12)$$

where $0 < r < s$ and $\mathfrak{a}(t = 0)$ is the dynamical activity:

$$\mathfrak{a}(t) \equiv \sum_{\mu', \mu (\mu \neq \mu')} W_{\mu'\mu} p_\mu(t). \quad (13)$$

Note that the dynamical activity $\mathfrak{a}(t)$ in Eq. (13) is a quantity of a single process [Eq. (3)]; the definition is the same as conventional Markov process settings. Dynamical activity was originally proposed as an order parameter in the study of glass transitions [42]. The dynamical activity plays a central cost term in thermodynamic trade-off relations [18, 20, 43, 44]. For $K = 1$, Eq. (12) reduces to the bound in Ref. [45]. While the right-hand side of Eq. (12) is written entirely in terms of quantities for a single process, the left-hand side contains the observable $N^{(\otimes K)}$ for the combined process of K replicas. Note that Eq. (12) is an intermediate relation that will be used to obtain trade-off relations in the single process. In other words, although we consider the combined process of replicas K, this is purely for mathematical purposes, and the final results that will be shown later are relations for the single process [cf. Eqs. (16) and (17)]. This is the same idea as in methods such as multi-copy measurements and the replica trick. As shown in the introduction, in two-copy measurements, we use $\rho\otimes\rho$ but the quantity obtained from using these copies is $\mathrm{Tr}[\rho^2]$, which is a quantity referring to the single-copy case. Considering $r=1$ and $s\to\infty$ in Eq. (12), we obtain

$$\mathbb{E}\left[\left|N^{(\otimes K)}\right|\right]\leq N_{\max}^{(\otimes K)}\left(1-e^{-\tau K\mathfrak{a}(t=0)}\right), \tag{14}$$

where $N_{\max}^{(\otimes K)}$ denotes the maximum value $N_{\max}^{(\otimes K)}\equiv\max_{\Gamma^{(\otimes K)}}\left|N^{(\otimes K)}(\Gamma^{(\otimes K)})\right|$. For $K=1$, the bound is identical to that reported in Ref. [45].

As mentioned above, by considering specific observables for $N^{(\otimes K)}$ in Eq. (14), we derive trade-off relations for a single process. In particular, this paper focuses on the Rényi entropy. For an arbitrary probability distribution p_n, the Rényi entropy with order α $(0<\alpha<\infty)$ is given by

$$H_\alpha[p_n]\equiv\frac{1}{1-\alpha}\ln\left(\sum_n p_n^\alpha\right). \tag{15}$$

The Rényi entropy is a one-parameter generalization of several entropies. The real parameter α is called the order of the Rényi entropy. By varying α, we can explore different aspects of uncertainty of the distribution. The Rényi entropies form a one-parameter family that continuously interpolate between several entropic definitions. In the limit $\alpha\to 0$, H_α approaches the max-entropy, which depends only on the number of outcomes with nonzero probability. In the limit $\alpha\to 1$, H_α reduces to the usual Shannon entropy. For $\alpha=2$, the Rényi entropy reduces to the collision entropy. In the limit $\alpha\to\infty$, H_α converges to the min-entropy, which is determined solely by the highest probability.

Entropic bound on network diffusion

As the first application of Eq. (14), we consider a random walker on a network, whose dynamics is governed by a continuous time Markov process [Eq. (3)], which is extensively investigated in the literature [46–48]. It has many applications in web search engines [49], community detection [50], embedding algorithms [51], and computational biology [52], to name but a few. We consider a continuous time random walk starting from the state B_{μ_0}. Here, we aim to quantify the extent of diffusion on the network (Fig. 2(a)). Typically, the mean squared displacement, mixing time, or spectral gap of the generator are used [46, 48]. Entropy is another metric used to quantify diffusion in a network. The diversity entropy [53, 54] is defined as the entropy of the walker's position probabilities and measures how widely a random walker can spread over the network. The entropy rate [55] quantifies how quickly uncertainty increases as the random walk evolves.

Let $p_\mu(\tau\mid\mu_0)$ be the probability of being in B_μ at time $t=\tau$ starting from the state B_{μ_0} at time $t=0$. In this case, the extent of diffusion from node μ_0 can be quantified by the Rényi entropy $H_\alpha[p_\mu(\tau\mid\mu_0)]$. When this Rényi entropy is zero, it indicates that no propagation has occurred in the network, and as the degree of propagation increases, the value of this Rényi entropy increases. Using Eq. (14), the following relation holds for the Rényi entropy (see Methods):

$$H_\alpha[p_\mu(\tau|\mu_0)]\leq\frac{\alpha\tau}{\alpha-1}\sum_{\mu(\mu\neq\mu_0)}W_{\mu\mu_0}\ \ (\alpha=2,3,\cdots), \tag{16}$$

which is the second result of this study. The left-hand side of Eq. (16) represents the Rényi entropy and it is bounded from above by the τ and the local escape rate from the initial node B_{μ_0}, which is the sum of the transition rates from the initial node B_{μ_0} to the nodes that can be reached within one jump. Note that $\sum_{\mu(\mu\neq\mu_0)}W_{\mu\mu_0}=\mathfrak{a}(t=0)$ corresponds to the dynamical activity at the initial time. Surprisingly, this right-hand side depends only on the time τ and on local escape rate from B_{μ_0} (see Fig. 3). In other words, regardless of how large the overall network is, we can compute the upper bound of the Rényi entropy using only information about the initial node and the transition rates to nodes that are reachable in a single hop. For integer values of α, $\alpha\in\{2,3,\cdots\}$, the relation is exact. Since the inequality of Eq. (16) still holds for real value of $\alpha>1$, we conjecture that this relation holds for arbitrary $\alpha>1$.

Entropic bound on trajectory observable

Next, we consider the uncertainty in trajectory observables. Trajectory observables play a fundamental role in uncertainty relations in stochastic thermodynamics (Fig. 2(b)). Consider a trajectory observable $N(\Gamma)$, which vanishes for $\Gamma_\varnothing$ [Eq. (11)]; that is, when there is no jump within $[0,\tau]$, the observable $N(\Gamma)$ vanishes. This is a generalization of counting observables often considered in stochastic thermodynamics. From Eq. (14), we obtain the following relation (see Methods):

$$H_\alpha[P(N)]\leq\frac{\alpha\tau}{\alpha-1}\mathfrak{a}(t=0)\ \ (\alpha=2,3,\cdots), \tag{17}$$

which is the third result of this study. The left-hand side of Eq. (17) is the Rényi entropy of the observable N, while the right-hand side depends on the dynamical activity and on the duration τ. For example, consider dynamics with no jumps at all, or the case $\tau=0$. Since there are no jumps, the distribution of N is $P(N=0)=1$, and the entropy of $N(\Gamma)$ is zero. In this case, the right-hand side also vanishes, so the result is consistent. On the other hand, for dynamics with a very large number of jumps, the distribution acquires weight at many different values of N, and the entropy increases. In fact, the right-hand side increases with both the dynamical activity and the duration τ, which matches our intuition. Note also

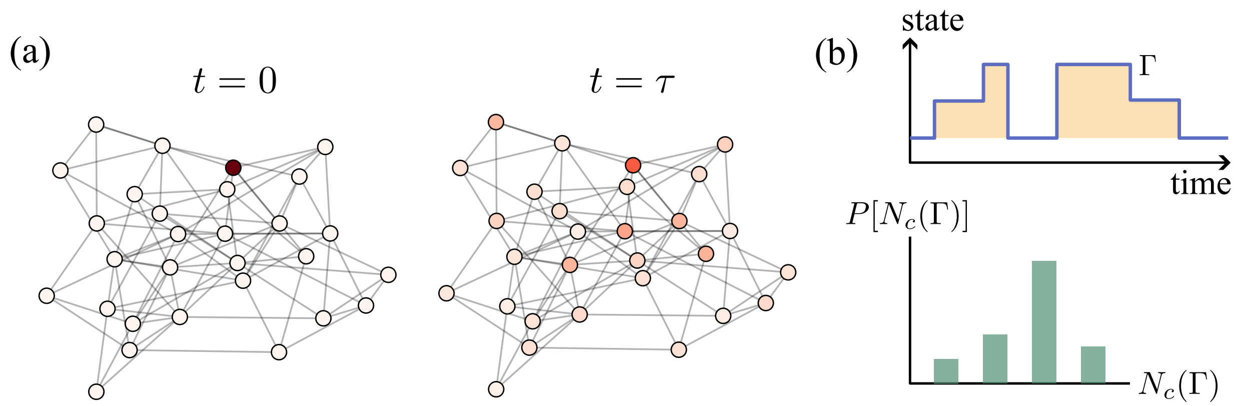

FIG. 2. Illustration of (a) the network diffusion bound [Eq. (16)] and (b) the trajectory observable bound [Eq. (17)]. (a) Diffusion in a random walk on a network. A random walker starts from a node in the network, which is represented by dark red. At time $t = \tau$, the random walker diffuses over the network and the probability $p_\mu(\tau)$ of the walker position is expressed by red, where darker color corresponds to higher probability. The network diffusion bound provides upper bound to the Rényi entropy of $p_\mu(\tau)$. (b) Trajectory observable bound in a Markov process. For the Rényi entropy bound for trajectory observables, we consider a trajectory Γ) and its associated observable $N(\Gamma)$. The Rényi entropy is calculated for the distribution $N(\Gamma)$.

that for the counting observable N, there is no upper bound on its possible values, and therefore there is no upper bound on the entropy either. For integer values of α, $\alpha \in \{2, 3, \cdots\}$, the relation is exact. Since the inequality of Eq. (17) formally holds for the real value of $\alpha > 1$, again, we conjecture that this relation holds for arbitrary $\alpha > 1$.

Traditionally, uncertainty in trajectory observables has been characterized using the variance $\mathrm{Var}[N]$, whose relative value is known to be bounded from below by the inverse of the dynamical activity. For a steady-state Markov process and the counting observable N_c, it is known that the following relation holds:

$$\frac{\mathrm{Var}[N_\mathrm{c}]}{\mathbb{E}[N_\mathrm{c}]^2} \geq \frac{1}{\mathfrak{a}_\mathrm{ss}\tau}, \tag{18}$$

where $\mathfrak{a}_\mathrm{ss}$ is the stead-state dynamical activity. Our results show that this fundamental constraint extends beyond relative variance: the uncertainty measure based on Rényi entropy is also limited by the dynamical activity. However, there is an important difference between Eq. (17) and Eq. (18). When the variance $\mathrm{Var}[N]$ decreases, the uncertainty in N becomes smaller; thus Eq. (18) provides a lower bound on the uncertainty in N. By contrast, Eq. (17) yields an upper bound on the uncertainty in N. Therefore, these two relations give complementary lower and upper bounds on the uncertainty of N, each expressed in terms of different quantities. The Rényi entropy reduces to the Shannon entropy for $\alpha \to 1$; however, the bound in Eq. (17) is not defined for $\alpha = 1$. Regarding the Shannon entropy for trajectory observables, Ref. [56] derived a lower bound for the Shannon entropy using the entropy production. The bound in Eq. (17) provides the upper bound of the Rényi entropy and the bound comprises the dynamical activity.

So far, we are concerned with the Rényi entropy for probability distributions. We can consider other observables to obtain trade-off relations by using replicas. We consider the variance:

$$V^{(\otimes 2)}(\Gamma^{(\otimes 2)}) = N^{(1)}(\Gamma^{(1)})^2 - N^{(1)}(\Gamma^{(1)})N^{(2)}(\Gamma^{(2)}). \tag{19}$$

Using the operator in Eq. (19), its expectation is

$$\mathbb{E}\left[V^{(\otimes 2)}(\Gamma^{(\otimes 2)})\right] = \mathbb{E}[N(\Gamma)^2] - \mathbb{E}[N(\Gamma)]^2 = \mathrm{Var}[N(\Gamma)]. \tag{20}$$

Assume that the minimum of $N(\Gamma)$ is 0. Substituting Eq. (20) into (14), we obtain the upper bound of the variance as follows:

$$\mathrm{Var}[N] \leq N_\mathrm{max}^2 \left(1 - e^{-2\tau\mathfrak{a}(t=0)}\right), \tag{21}$$

where N_max is the maximum $N_\mathrm{max} \equiv \max_\Gamma |N(\Gamma)|$. Equation (21) gives an upper bound on the observable N. To make the discussion concrete, let us focus on the counting observable N_c. If no jump occurs, the right-hand side of Eq. (21) vanishes, and the variance of N_c is also zero, so the bound is satisfied. However, for typical counting observables there is no upper limit on the number of jumps, so $N_\mathrm{max} = \infty$, and Eq. (21) is no longer applicable. In contrast, when we consider qudits and related finite-dimensional systems, which are often used as working media in heat engines, the observable is naturally bounded. In such cases N_max is finite, and Eq. (21) provides a meaningful bound.

Numerical simulation

We perform numerical calculations for the diffusion bound of a random walker in a network [Eq. (16)]. We generate a random network and consider a continuous

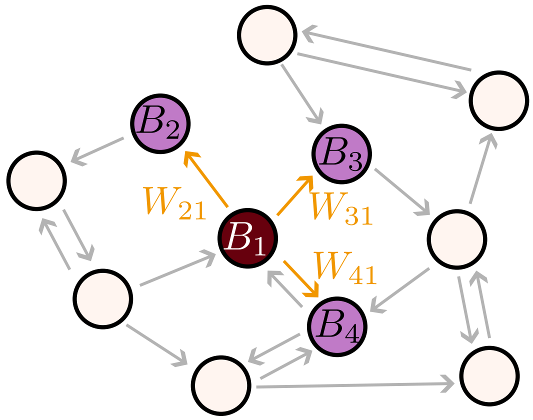

FIG. 3. Illustration of the dependence of the Rényi entropic bound. The Rényi entropic bound for the network diffusion depends on $\sum_{\mu(\mu\neq\mu_0)} W_{\mu\mu_0}$, where B_{μ_0} is the initial state, the local escape rate from B_{μ_0}. The local escape rate from B_{μ_0} is the sum of transition rates to which the nodes reachable from the initial state with one jump. Suppose the initial state is B_1, which is colored with dark red. Then, the reachable states are represented by purple nodes. Therefore, the local escape rate becomes $\sum_{\mu(\mu\neq\mu_0)} W_{\mu\mu_0} = W_{21} + W_{31} + W_{41}$.

time random walk on the network. The transition rate $W_{\mu'\mu}$ and the initial node are chosen randomly. We calculate the probability distribution at time $t = \tau$, where τ is determined randomly. The range for these random parameters is shown in the caption of Fig. 4. We repeat this procedure to obtain random realizations and calculate the Rényi entropy (the left-hand side of Eq. (16)) and $\sum_{\mu(\mu\neq\mu_0)} W_{\mu\mu_0}$ (the right-hand side of Eq. (16)). For each random realization, we plot $H_\alpha[p_\mu(\tau)]$ versus $\frac{\alpha\tau}{\alpha-1}\sum_{\mu(\mu\neq\mu_0)} W_{\mu\mu_0}$ as a point in Fig. 4, where the dashed line indicates the equality case in Eq. (16). In Figs. 4(a)-(c), we plot the results for (a) $\alpha = 1.5$, (b) $\alpha = 2$, and (c) $\alpha = 3$. For all values of α, the points lie above the dashed line, providing numerical verification of Eq. (16). The bound is quite tight, especially for larger α. Note that for $\alpha = 2$ and 3, Eq. (16) is exact. However, for a non-integer α, the relation has not been proven, so Eq. (16) in $\alpha = 1.5$ should be regarded as a conjecture. Our numerical simulations indicate that this conjectured bound also holds in the non-integer case.

Next, we perform numerical calculations for the bound for the trajectory observable [Eq. (17)]. We generate a continuous time Markov process, where the transition rate $W_{\mu'\mu}$ and the initial probability distribution $p_\mu(0)$ are determined randomly. We consider the counting observable $N_{\mathrm{c}}(\Gamma)$, which simply counts the number of total jumps within the interval $[0,\tau]$, where τ is randomly determined. The range for these random parameters is shown in the caption of Fig. 4. We repeat this procedure to obtain random realizations and calculate the Rényi entropy and the dynamical activity. For each random realization, we plot $H_\alpha[P(N)]$ versus $\frac{\alpha\tau\mathfrak{a}(t=0)}{\alpha-1}$ by a point in Fig. 5. In Figs. 5(a)-(c), we plot the results for (a) $\alpha = 1.5$, (b) $\alpha = 2$, and (c) $\alpha = 3$, where the dashed line denotes the equality case of Eq. (17). Again, in all cases of α, the points are above the dashed line, which numerically verifies Eq. (17). The derived relation numerically holds for $\alpha = 1.5$, which is non-integer and is a conjectured bound.

Quantum generalization

The bounds given in Eqs. (12) and(14) can be generalized to quantum scenarios using the continuous measurement formalism. Let $\rho(t)$ denote the density operator of the system at time t. We assume that its dynamics are governed by a Lindblad master equation:

$$\dot{\rho}(t) = \mathcal{L}\rho(t), \tag{22}$$

where the Lindblad generator $\mathcal{L}$ is given by

$$\mathcal{L}\rho \equiv -i[H,\rho] + \sum_{m=1}^{\mathfrak{N}} \mathcal{D}[L_m]\rho. \tag{23}$$

Here, H is the system Hamiltonian, L_m is the m-th jump operator, $\mathfrak{N}$ is the number of jump channels, and

$$\mathcal{D}[L]\rho \equiv L\rho L^\dagger - \frac{1}{2}\{L^\dagger L, \rho\}, \tag{24}$$

is the corresponding dissipator. The jump operators L_m describe dissipative processes such as energy relaxation, dephasing, and decoherence. Each term represents a distinct decay or noise channel through which the system interacts with its environment. The term $-i[H,\rho]$ in Eq. (23) generates the coherent part of the evolution, while the dissipators $\mathcal{D}[L_m]$ represent irreversible, non-unitary dynamics induced by this coupling. The Lindblad form of $\mathcal{L}$ guarantees that the time evolution is completely positive and trace preserving (CPTP). Equation (22) provides a general description of Markovian open quantum system dynamics. When the dynamics are restricted to the energy eigenbasis, that is, when the initial state and the jump operators do not include off-diagonal contributions with respect to the energy eigenbasis, the dynamics reduce to the classical Markov process expressed by Eq. (3).

We now consider continuous measurement in the Lindblad framework, corresponding to continuous monitoring of the environment coupled to the system (see Ref. [57]). In this setting, the system's stochastic evolution is conditioned on the measurement outcomes registered in the environment, and individual realizations of the dynamics are described by quantum trajectories. The measurement record consists of the types of jump events and their time stamps, which represent the full history of detected quanta (such as emitted photons or transferred particles) over the time interval. Suppose that within the interval $[0,\tau]$ there are J jump events, and let $m_j \in \{1,\ldots,\mathfrak{N}\}$

denote the type of the j-th jump occurring at time t_j. The full measurement record is

$$\Gamma_{\mathrm{q}} \equiv \left[(t_1, m_1), (t_2, m_2), \ldots, (t_J, m_J)\right], \quad (25)$$

where the subscript q is used to emphasize that Γ_{q} is a quantum trajectory. The sequence Γ_{q} characterizes one realization of the monitored dynamics and is the basic object from which we construct trajectory-dependent observables. Consider a trajectory observable $N_{\mathrm{q}}(\Gamma_{\mathrm{q}})$. Let $\Gamma_{\mathrm{q}\varnothing}$ be arbitrary quantum trajectory, where there is no jump within the interval $[0, \tau]$. Analogous to the condition of Eq. (11), we assume that $N_{\mathrm{q}}(\Gamma_{\mathrm{q}})$ satisfies the following condition:

$$N_{\mathrm{q}}(\Gamma_{\mathrm{q}\varnothing}) = 0. \quad (26)$$

N_{q} includes counting observables, which simply count the number of jumps. In a similar manner to the classical case, we consider K replicas of the identical quantum Markov process. A quantum trajectory of $K = 2$ replicas is

$$\Gamma_{\mathrm{q}}^{(\otimes 2)} = \Gamma_{\mathrm{q}}^{(\otimes 2)}\left(\Gamma_{\mathrm{q}}^{(1)}, \Gamma_{\mathrm{q}}^{(2)}\right), \quad (27)$$

where $\Gamma_{\mathrm{q}}^{(1)}$ and $\Gamma_{\mathrm{q}}^{(2)}$ trajectories in the first and the second processes, respectively. It is straightforward to generalize to K-replica scenario, in which the corresponding trajectory is expressed as $\Gamma_{\mathrm{q}}^{(\otimes K)}$.

It is possible to consider a quantum generalization of the dynamical activity given in Eq. (13). The classical dynamical activity [Eq. (13)] quantifies the extent of activity of the dynamics. For classical Markov processes, the state change occurs only when there are jumps. However, for the quantum scenario, the state change can occur even without jumps due to the coherent contribution arising from $-i[H, \rho]$ term in Eq. (23). Let $\mathcal{B}(\tau)$ be the quantum dynamical activity within the interval $[0, \tau]$. The quantum dynamical activity plays a central role in trade-off relations in quantum thermodynamics [32, 44, 58–60]. For the explicit expression of $\mathcal{B}(\tau)$, please see the Methods. It can be shown that the trajectory observable $N_{\mathrm{q}}(\Gamma_{\mathrm{q}})$ satisfies the following relation (see Methods):

$$\frac{\mathbb{E}\left[|N_{\mathrm{q}}^{(\otimes K)}|^s\right]^{r/(s-r)}}{\mathbb{E}\left[|N_{\mathrm{q}}^{(\otimes K)}|^r\right]^{s/(s-r)}} \geq \left(1 - \cos\left[\frac{1}{2}\int_0^\tau \frac{\sqrt{\mathcal{B}(t)}}{t} dt\right]^{2K}\right)^{-1}, \quad (28)$$

where $0 \leq (1/2)\int_0^\tau \sqrt{\mathcal{B}(t)}/t\, dt \leq \pi/2$. Similarly to the classical counterpart [Eq. (12)], the right-hand side of Eq. (28) depends on the quantum dynamical activity $\mathcal{B}(\tau)$. For the classical case, the right-hand side depends solely on the initial dynamical activity $\mathfrak{a}(t = 0)$. On the other hand, $\mathcal{B}(\tau)$ depends on dynamics within the interval $[0, \tau]$. Again, by considering $r = 1$ and $s \to \infty$ in Eq. (28) we obtain

$$\mathbb{E}\left[|N_{\mathrm{q}}^{(\otimes K)}|\right] \leq N_{\mathrm{q\,max}}^{(\otimes K)}\left(1 - \cos\left[\frac{1}{2}\int_0^\tau \frac{\sqrt{\mathcal{B}(t)}}{t} dt\right]^{2K}\right), \quad (29)$$

where $N_{\mathrm{q\,max}}^{(\otimes K)} \equiv \max_{\Gamma_{\mathrm{q}}^{(\otimes K)}} |N_{\mathrm{q}}^{(\otimes K)}(\Gamma_{\mathrm{q}}^{(\otimes K)})|$ and $0 \leq (1/2)\int_0^\tau \sqrt{\mathcal{B}(t)}/t\, dt \leq \pi/2$.

Let us consider the probability distribution of $N_{\mathrm{q}}(\Gamma)$. Similarly to the classical case, we can derive upperbound to the Rényi entropy of $P(N_{\mathrm{q}})$. From Eq. (29), we obtain the following relation (see Methods):

$$H_\alpha[P(N_{\mathrm{q}})] \leq \frac{2\alpha}{1-\alpha} \ln\cos\left[\frac{1}{2}\int_0^\tau \frac{\sqrt{\mathcal{B}(t)}}{t} dt\right], \quad (30)$$

where $\alpha = 2, 3, \cdots$. Equation (30) is a quantum generalization of Eq. (17). The left-hand side of Eq. (17) is the Rényi entropy of the observable N_{q}, while the right-hand side depends on the quantum dynamical activity $\mathcal{B}(\tau)$. For integer values of α, $\alpha \in \{2, 3, \cdots\}$, the relation is exact. Since the inequality of Eq. (17) formally holds for the real value of $\alpha > 1$, we conjecture that this relation holds for arbitrary $\alpha > 1$.

DISCUSSION

We have introduced replica Markov processes as a tool to derive thermodynamic trade-off relations for nonlinear functions of probability distributions. Entropic quantities such as Rényi entropies are nonlinear and are therefore harder to handle. By considering K replica processes, we derived a replica trade-off relation that lower-bounds relative moments of trajectory observables by a term expressed by the dynamical activity [Eq. (12)].

We then showed how this replica trade-off relation can be converted into entropic bounds for a single Markov process. First, for a continuous-time random walk on a network, we obtained an upper bound on the Rényi entropy of the position distribution at time τ [Eq. (16)]. Remarkably, the bound depends only on τ and the local escape rate from the initial node, i.e., the sum of transition rates to nodes reachable in one hop. This provides an information-theoretic constraint on network diffusion that is computable from purely local data, independent of the global network size or structure. Second, for trajectory observables, we derived an upper bound on the Rényi entropy of the observable distribution [Eq. (17)] in terms of the dynamical activity. This gives an entropic characterization of trajectory-level uncertainty that complements and conceptually generalizes variance-based thermodynamic uncertainty relations.

We also discussed a direct quantum extension within the continuous-measurement quantum trajectory framework. The resulting replica inequality involves the quan-

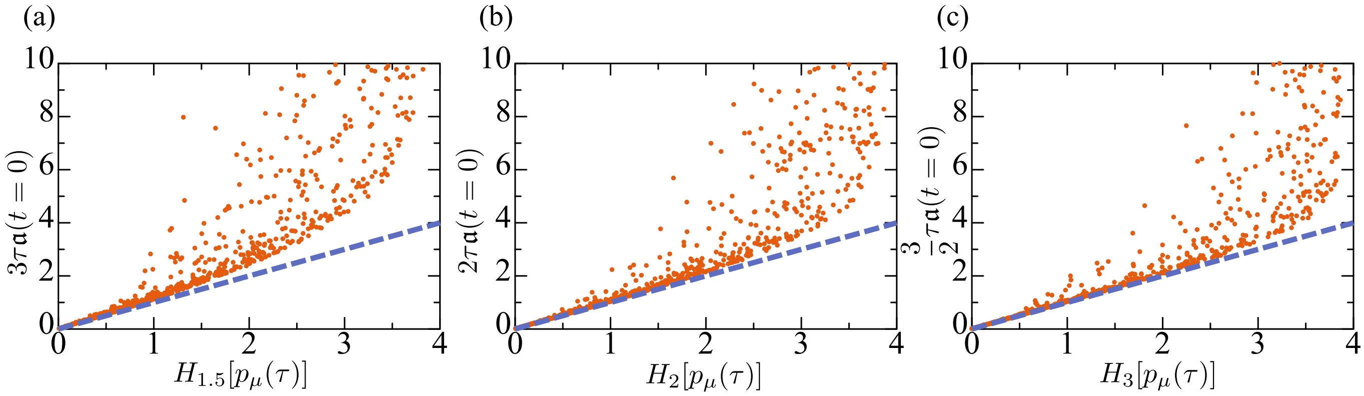

FIG. 4. Numerical verification of the Rényi entropy bound in Eq. (16). The Rényi entropy $H_\alpha[p_\mu(\tau)]$ versus $\frac{\alpha\tau}{\alpha-1}\sum_{\mu(\mu\neq\mu_0)} W_{\mu\mu_0}$ is plotted for (a) $\alpha = 1.5$, (b) $\alpha = 2$, and (c) $\alpha = 3$. Random realizations are shown with points and the dashed line indicates the equality case of Eq. (16). In (a)-(c), the simulations begin by selecting the number of state D between 3 and 50. Then, the transition rate $W_{\mu'\mu}$ is randomly produced, and τ is chosen within the range of 0.1 to 10.

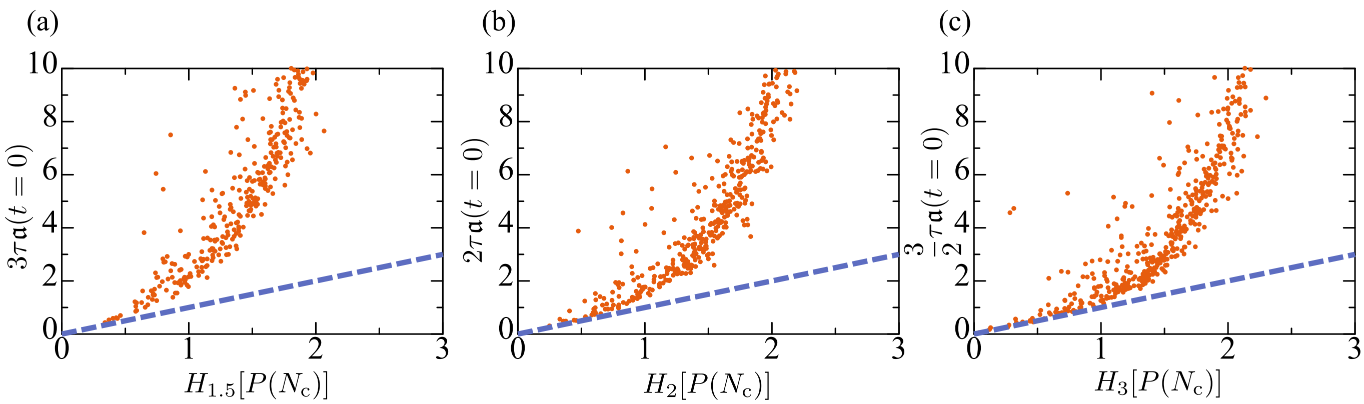

FIG. 5. Numerical verification of the Rényi entropy bound in Eq. (17). The Rényi entropy $H_\alpha[P(N_c)]$ versus $\alpha\tau\mathfrak{a}(t=0)/(\alpha-1)$ is plotted for (a) $\alpha = 1.5$, (b) $\alpha = 2$, and (c) $\alpha = 3$. Random realizations are shown with points and the solid line indicates the equality case of Eq. (17). In (a)-(c), classical simulations begin by selecting the number of states D between 2 and 5. Then, the transition rate $W_{\mu'\mu}$ is randomly produced, and τ is chosen within the range of 0.1 to 10. The observable $N_c(\Gamma)$ is the number of total jumps within $[0,\tau]$. The Rényi entropy of the observable is estimated by averaging the results of 10^3 simulations.

tum dynamical activity, capturing both jump and coherent contributions, and leads to an entropic bound for quantum counting observables [Eq. (28)].

METHODS

A. Derivation of Eq. (12)

The derivation of the main result [Eq. (12)] is based on Ref. [45] and we extend the bound to the case including K replicas.

First, we consider the single-process case. The probability of the trajectory Γ [Eq. (4)] is given by [61]

$$\mathcal{P}(\Gamma) = p_\mu(t=0)\mathcal{P}(\Gamma \mid \mu_0), \tag{31}$$

where $\mathcal{P}(\Gamma \mid \mu_0)$ is the trajectory probability given that the initial state is B_{μ_0} and $X_j = B_{\mu_j}$:

$$\mathcal{P}(\Gamma \mid \mu_0) = \prod_{j=1}^{J} W_{\mu_j\mu_{j-1}} e^{-\sum_{j=0}^{J}(t_{j+1}-t_j)R(\mu_j)}, \tag{32}$$

where $t_{J+1} \equiv \tau$. Here, $R(\mu)$ is defined by

$$R(\mu) \equiv \sum_{\mu'(\neq\mu)} W_{\mu'\mu}. \tag{33}$$

Let $\mathfrak{p}(\tau)$ be the probability that there is no jump within the interval $[0,\tau]$. From Eq. (31), $\mathfrak{p}(\tau)$ is expressed as

$$\mathfrak{p}(\tau) = \sum_{\mu_0} p_{\mu_0}(t=0)e^{-\tau R(\mu_0)}. \tag{34}$$

Using the Jensen inequality, we obtain

$$\begin{aligned}\mathfrak{p}(\tau) &\geq e^{-\tau\sum_{\mu_0} p_{\mu_0}(t=0)R(\mu_0)} \\ &= e^{-\tau\mathfrak{a}(t=0)}.\end{aligned} \tag{35}$$

Next, we consider the trajectory $\Gamma^{(\otimes K)}$ in the K replica processes. Let $\mathfrak{p}^{(\otimes K)}(\tau)$ be the probability that there is no jump within the interval $[0,\tau]$ in the K replica case. Since the replicas are independent processes, from Eq. (35), $\mathfrak{p}^{(\otimes K)}(\tau)$ is bounded from below by

$$\mathfrak{p}^{(\otimes K)}(\tau) \geq \left[e^{-\tau\sum_{\mu_0} p_{\mu_0}(t=0)R(\mu_0)}\right]^K = e^{-K\tau\mathfrak{a}(t=0)}. \tag{36}$$

We can relate $\mathfrak{p}^{(\otimes K)}(\tau)$ to the probability $P\left[N^{(\otimes K)}(\Gamma^{(\otimes K)})=0\right]$, which is the probability that the observable $N^{(\otimes K)}$ vanishes. If no jump occurs in the interval $[0,\tau]$, then the observable satisfies $N^{(\otimes K)}(\Gamma^{(\otimes K)}) = 0$ by the condition in Eq. (11). The converse, however, does not necessarily hold. Therefore, the probability that $N^{(\otimes K)}(\Gamma^{(\otimes K)}) = 0$ is bounded from below by

$$P\left[N^{(\otimes K)}(\Gamma^{(\otimes K)})=0\right] \geq \mathfrak{p}^{(\otimes K)}(\tau). \tag{37}$$

Let X be a random variable. According to Ref. [62], the following relation holds:

$$P(|X|>b) \geq \frac{\left(\mathbb{E}\left[|X|^r\right]-b^r\right)^{s/(s-r)}}{\mathbb{E}\left[|X|^s\right]^{r/(s-r)}}, \tag{38}$$

where $0<r<s, b\geq 0$ and $b^r \leq \mathbb{E}\left[|X|^r\right]$ should be satisfied. Using Eq. (38) with $b=0$ for the random variable $N^{(\otimes K)}$, we obtain

$$\begin{aligned}\frac{\mathbb{E}\left[|N^{(\otimes K)}|^r\right]^{s/(s-r)}}{\mathbb{E}\left[|N^{(\otimes K)}|^s\right]^{r/(s-r)}} &\leq P(|N^{(\otimes K)}|>0) \\ &= 1-P(|N^{(\otimes K)}|=0) \\ &\leq 1-\mathfrak{p}^{(\otimes K)}(\tau) \\ &\leq 1-e^{-K\tau\mathfrak{a}(t=0)},\end{aligned} \tag{39}$$

where we used Eqs. (37) and (36). Equation (39) is Eq. (12). Taking $s\to\infty$ and $r=1$, we have

$$\mathbb{E}\left[|N^{(\otimes K)}|^s\right]^{r/(s-r)} = \max_{\Gamma^{(\otimes K)}} |N^{(\otimes K)}(\Gamma^{(\otimes K)})|. \tag{40}$$

Using Eq. (40) in Eq. (39), we obtain Eq. (14) in the main text.

B. Derivation of Eqs. (16) and (17)

We show the derivation of Eqs. (16) and (17). We consider the particular observable for $N^{(\otimes K)}$ to obtain inequalities for the original single process. Specifically, let us consider the following observable:

$$\Lambda^{(\otimes 2)}(\Gamma^{\otimes 2}) \equiv \begin{cases} 0 & N^{(1)}(\Gamma^{(1)}) = N^{(2)}(\Gamma^{(2)}) \\ 1 & \text{otherwise}\end{cases}. \tag{41}$$

$\Lambda^{(\otimes 2)}$ is interpreted as follows. Consider the trajectories $\Gamma^{(1)}$ and $\Gamma^{(2)}$ of two independent processes, and take the observable $N^{(k)}(\Gamma^{(k)})$, defined in Eq. (11), on these two processes. Then $\Lambda^{(\otimes 2)}$ returns 0 only when the values of the observable N in the two processes agree, $N^{(1)}(\Gamma^{(1)}) = N^{(2)}(\Gamma^{(2)})$. When there is no jump in the first and second processes, we trivially obtain $N^{(1)}(\Gamma^{(1)}_\varnothing) = N^{(2)}(\Gamma^{(2)}_\varnothing) = 0$. Then the observable $\Lambda^{(\otimes 2)}$ satisfies

$$\Lambda^{(\otimes 2)}(\Gamma^{\otimes 2}_\varnothing) = 0, \tag{42}$$

which is the condition of Eq. (11). Let $\mathcal{Z}$ be the set of all possible values that the observable $N(\Gamma)$ can take. Then, the expectation becomes the following:

$$\begin{aligned}&\mathbb{E}\left[\Lambda^{(\otimes 2)}(\Gamma^{\otimes 2})\right] \\ &= 1-\sum_{z\in\mathcal{Z}} P(N^{(1)}(\Gamma^{(1)})=z)P(N^{(2)}(\Gamma^{(2)})=z) \\ &= 1-\sum_{z\in\mathcal{Z}} P(N(\Gamma)=z)^2.\end{aligned} \tag{43}$$

Moreover, since $\Lambda^{(\otimes 2)}$ returns either 1 or 0, we have

$$[\Lambda^{(\otimes 2)}(\Gamma^{\otimes 2})]_{\max} = 1. \tag{44}$$

Substituting Eqs. (43) and (44) into Eq. (14), we obtain

$$\sum_{z\in\mathcal{Z}} P(N(\Gamma)=z)^2 \geq e^{-2\tau\mathfrak{a}(t=0)}. \tag{45}$$

The derivation above was presented for the case $K=2$. It can be straightforwardly extended to any integer $K\geq 2$, yielding

$$\sum_{z\in\mathcal{Z}} P(N(\Gamma)=z)^K \geq e^{-K\tau\mathfrak{a}(t=0)}, \tag{46}$$

which derives Eq. (17) in the main text.

Next, we consider the following observable:

$$\Xi^{(\otimes 2)}(\Gamma^{\otimes 2}) \equiv \begin{cases} 0 & X^{(1)}(\tau) = X^{(2)}(\tau) \\ 1 & \text{otherwise}\end{cases}. \tag{47}$$

Here, $X^{(k)}(\tau)$ is the state of the k-th process at time $t=\tau$. Therefore, Eq. (47) is 0 if the final state of the first and the second processes agree. In this study, when considering a random walker on a network, we assume that the initial state of the random walk is B_{μ_0}. This implies that, when there is no jump within the interval $[0,\tau]$, the final state at time $t=\tau$ is $X^{(1)}(\tau) = X^{(2)}(\tau) = B_{\mu_0}$. Therefore, the observable $\Xi^{(\otimes 2)}$ satisfies

$$\Xi^{(\otimes 2)}(\Gamma^{(\otimes 2)}_\varnothing) = 0, \tag{48}$$

which satisfies the condition given in Eq. (11). The expectation of $\Xi^{(\otimes 2)}$ is given by

$$\begin{aligned}&\mathbb{E}\left[\Xi^{(\otimes 2)}(\Gamma^{(\otimes 2)})\right] \\ &= 1-\sum_{\mu} P(X^{(1)}(\tau)=B^{(1)}_\mu)P(X^{(2)}(\tau)=B^{(2)}_\mu) \\ &= 1-\sum_\mu p_\mu(\tau)^2.\end{aligned} \tag{49}$$

Again, the maximum of $\Xi^{(\otimes 2)}$ is given by

$$[\Xi^{(\otimes 2)}(\Gamma^{\otimes 2})]_{\max} = 1. \tag{50}$$

Substituting Eqs. (49) and (50) into Eq. (14), we obtain

$$\sum_{\mu} p_\mu(\tau)^2 \geq e^{-2\tau\mathfrak{a}(t=0)}. \tag{51}$$

The derivation above was presented for the case $K = 2$. It can be straightforwardly extended to any integer $K \geq 2$, yielding

$$\sum_{\mu} p_\mu(\tau)^K \geq e^{-K\tau\mathfrak{a}(t=0)}, \tag{52}$$

which derives Eq. (16) in the main text.

C. Derivation of Eq. (28)

We show the derivation of Eq. (28), which is the quantum generalization of Eq. (12). Similarly to the classical case, let $\mathfrak{p}_\mathrm{q}(\tau)$ be the probability that there is no jump within the interval $[0,\tau]$ in Γ_q. From the result in Ref. [45], the following relation holds:

$$\cos\left[\frac{1}{2}\int_0^\tau \frac{\sqrt{\mathcal{B}(t)}}{t}dt\right]^2 \leq \mathfrak{p}_\mathrm{q}(\tau), \tag{53}$$

where the following condition should be met:

$$0 \leq \frac{1}{2}\int_0^\tau \frac{\sqrt{\mathcal{B}(t)}}{t}dt \leq \frac{\pi}{2}. \tag{54}$$

We consider the K replica scenario, where there are K identical processes. Let $\mathfrak{p}_\mathrm{q}^{(\otimes K)}(\tau)$ denote the probability that there is no jump in the K replica processes. Since each process is independent, from Eq. (53), $\mathfrak{p}_\mathrm{q}^{(\otimes K)}(\tau)$ satisfies

$$\cos\left[\frac{1}{2}\int_0^\tau \frac{\sqrt{\mathcal{B}(t)}}{t}dt\right]^{2K} \leq \mathfrak{p}_\mathrm{q}^{(\otimes K)}(\tau). \tag{55}$$

If no jump occurs in the interval $[0,\tau]$, then the observable satisfies $N_\mathrm{q}^{(\otimes K)}(\Gamma_\mathrm{q}^{(\otimes K)}) = 0$ by the condition in Eq. (26). The converse, however, does not necessarily hold. Therefore, the probability that $N_\mathrm{q}^{(\otimes K)}(\Gamma_\mathrm{q}^{(\otimes K)}) = 0$ is bounded from below by

$$P\left[N_\mathrm{q}^{(\otimes K)}(\Gamma_\mathrm{q}^{(\otimes K)}) = 0\right] \geq \mathfrak{p}_\mathrm{q}^{(\otimes K)}(\tau). \tag{56}$$

Using the Petrov inequality [Eq. (38)], we have

$$\begin{aligned}
&\frac{\mathbb{E}\left[|N_\mathrm{q}^{(\otimes K)}|^r\right]^{s/(s-r)}}{\mathbb{E}\left[|N_\mathrm{q}^{(\otimes K)}|^s\right]^{r/(s-r)}} \\
&\leq P(|N_\mathrm{q}^{(\otimes K)}| > 0) \\
&= 1 - P(|N_\mathrm{q}^{(\otimes K)}| = 0) \\
&\leq 1 - \mathfrak{p}_\mathrm{q}^{(\otimes K)}(\tau) \\
&\leq 1 - \cos\left[\frac{1}{2}\int_0^\tau \frac{\sqrt{\mathcal{B}(t)}}{t}dt\right]^{2K}.
\end{aligned} \tag{57}$$

where we used Eqs. (55) and (56). Equation (57) proves Eq. (28) in the main text. Similarly to Eq. (40), taking $s \to \infty$ and $r = 1$, we have

$$\mathbb{E}\left[|N_\mathrm{q}^{(\otimes K)}|^s\right]^{r/(s-r)} = \max_{\Gamma_\mathrm{q}^{(\otimes K)}} |N_\mathrm{q}^{(\otimes K)}(\Gamma_\mathrm{q}^{(\otimes K)})|. \tag{58}$$

By using Eq. (58) in Eq. (57), we reproduce Eq. (29).

D. Derivation of Eq. (30)

We show the derivation of Eq. (30), which directly parallels the derivation of Eq.(17). Specifically, let us consider the following observable:

$$\Lambda_\mathrm{q}^{(\otimes 2)}(\Gamma_\mathrm{q}^{\otimes 2}) \equiv \begin{cases} 0 & N_\mathrm{q}^{(1)}(\Gamma_\mathrm{q}^{(1)}) = N_\mathrm{q}^{(2)}(\Gamma_\mathrm{q}^{(2)}) \\ 1 & \text{otherwise} \end{cases}. \tag{59}$$

Then $\Lambda_\mathrm{q}^{(\otimes 2)}$ returns 0 only when the values of the observable N_q in the two processes agree, $N_\mathrm{q}^{(1)}(\Gamma_\mathrm{q}^{(1)}) = N_\mathrm{q}^{(2)}(\Gamma_\mathrm{q}^{(2)})$. Then the observable $\Lambda_\mathrm{q}^{(\otimes 2)}$ satisfies

$$\Lambda_\mathrm{q}^{(\otimes 2)}(\Gamma_{\mathrm{q}\varnothing}^{\otimes 2}) = 0, \tag{60}$$

which is the condition of Eq. (26). Let $\mathcal{Z}_\mathrm{q}$ be the set of all possible values that the observable $N_\mathrm{q}(\Gamma_\mathrm{q})$ can take. Then, the expectation becomes the following:

$$\begin{aligned}
&\mathbb{E}\left[\Lambda_\mathrm{q}^{(\otimes 2)}(\Gamma_\mathrm{q}^{\otimes 2})\right] \\
&= 1 - \sum_{z\in\mathcal{Z}_\mathrm{q}} P(N_\mathrm{q}^{(1)}(\Gamma_\mathrm{q}^{(1)}) = z)P(N_\mathrm{q}^{(2)}(\Gamma_\mathrm{q}^{(2)}) = z) \\
&= 1 - \sum_{z\in\mathcal{Z}_\mathrm{q}} P(N_\mathrm{q}(\Gamma_\mathrm{q}) = z)^2.
\end{aligned} \tag{61}$$

Moreover, since $\Lambda^{(\otimes 2)}$ returns either 1 or 0, we have

$$[\Lambda_\mathrm{q}^{(\otimes 2)}(\Gamma_\mathrm{q}^{\otimes 2})]_{\max} = 1. \tag{62}$$

By considering a general K case and substituting Eqs. (61) and (62) into Eq. (29), we obtain

$$\sum_{z\in\mathcal{Z}_\mathrm{q}} P(N_\mathrm{q}(\Gamma_\mathrm{q}) = z)^K \geq \cos\left[\frac{1}{2}\int_0^\tau \frac{\sqrt{\mathcal{B}(t)}}{t}dt\right]^{2K}, \tag{63}$$

which derives Eq. (30) in the main text.

E. Quantum dynamical activity

We briefly review the quantum dynamical activity, a quantum generalization of the dynamical activity defined in Eq. (13).

First, we show how the classical dynamical activity defined in Eq. (13) can be expressed using the Lindblad equation. Using the jump operators L_m, the dynamical activity can be written as

$$\mathcal{A}(\tau) \equiv \int_0^\tau \sum_m \mathrm{Tr}\left[L_m \rho(t) L_m^\dagger\right] dt. \tag{64}$$

In the classical limit, this expression reduces to the classical dynamical activity:

$$\mathcal{A}_{\mathrm{cl}}(\tau) = \int_0^\tau \mathfrak{a}(t) dt = \int_0^\tau \sum_{\mu',\mu(\mu\neq\mu')} W_{\mu'\mu} p_\mu(t) dt. \tag{65}$$

Next, we consider a quantum generalization of the dynamical activity. The quantum dynamical activity plays a central role in trade-off relations [32, 44, 58–60, 63]. The exact expression for $\mathcal{B}(t)$ in the quantum dynamical activity was recently obtained in Refs. [58, 59]. Specifically, Ref. [59] showed the following relation:

$$\mathcal{B}(\tau) = \mathcal{A}(\tau) + \mathcal{C}(\tau), \tag{66}$$

where $\mathcal{C}(\tau)$ is the contribution from coherent dynamics,

$$\begin{aligned}\mathcal{C}(\tau) \equiv 8 \int_0^\tau ds_1 \int_0^{s_1} ds_2 \mathrm{Re}\left[\mathrm{Tr}\{H_{\mathrm{eff}}^\dagger \check{H}(s_1 - s_2)\rho(s_2)\}\right] \\ - 4\left(\int_0^\tau ds\, \mathrm{Tr}\left[H\rho(s)\right]\right)^2.\end{aligned} \tag{67}$$

Here, $\check{H}(t) \equiv e^{\mathcal{L}^\dagger t} H$ is the Hamiltonian H in the Heisenberg picture, and $\mathcal{L}^\dagger$ is the adjoint Liouvillian,

$$\mathcal{L}^\dagger \mathcal{O} \equiv i\,[H, \mathcal{O}] + \sum_{m=1}^{\mathfrak{N}} \mathcal{D}^\dagger[L_m]\mathcal{O}, \tag{68}$$

with $\mathcal{D}^\dagger$ the adjoint dissipator,

$$\mathcal{D}^\dagger[L]\mathcal{O} \equiv L^\dagger \mathcal{O} L - \frac{1}{2}\{L^\dagger L, \mathcal{O}\}, \tag{69}$$

for an operator $\mathcal{O}$.

As discussed above, the classical dynamical activity quantifies how frequently the system undergoes jumps and can be obtained from jump statistics. The quantum dynamical activity extends this notion to quantum Markov processes. In such processes, the system state can change even in the absence of jumps because of coherent evolution generated by H, and $\mathcal{C}(\tau)$ in Eq. (66) captures this purely coherent contribution. In the classical limit $H = 0$, we have $\mathcal{C}(\tau) = 0$ and thus $\mathcal{B}(\tau) = \mathcal{A}(\tau)$.

Under steady-state conditions, the classical dynamical activity grows linearly in time, $\mathcal{A}(\tau) = \mathfrak{a}_{\mathrm{ss}}\tau$. By contrast, the quantum dynamical activity can exhibit superlinear growth over a finite time interval, even in the steady state, due to coherent dynamics [59]. For large times, however, $\mathcal{B}(\tau)$ again becomes linear in τ: in Ref. [32], the asymptotic form of $\mathcal{B}(\tau)$ for $\tau \to \infty$ was derived.

ACKNOWLEDGMENTS

This work was supported by JSPS KAKENHI Grant Numbers JP23K24915 and JP24K03008.

[1] A. K. Ekert, C. M. Alves, D. K. L. Oi, M. Horodecki, P. Horodecki, and L. C. Kwek, Direct estimations of linear and nonlinear functionals of a quantum state, Phys. Rev. Lett. **88**, 217901 (2002).

[2] S. Aaronson, Shadow tomography of quantum states, Proc. STOC , 325 (2018).

[3] H.-Y. Huang, R. Kueng, and J. Preskill, Predicting many properties of a quantum system from very few measurements, Nat. Phys. **16**, 1050 (2020).

[4] A. Elben, S. T. Flammia, H.-Y. Huang, R. Kueng, J. Preskill, B. Vermersch, and P. Zoller, The randomized measurement toolbox, Nat. Rev. Phys. **5**, 9 (2023).

[5] M. Larocca, S. Thanasilp, S. Wang, K. Sharma, J. Biamonte, P. J. Coles, L. Cincio, J. R. McClean, Z. Holmes, and M. Cerezo, Barren plateaus in variational quantum computing, Nat. Rev. Phys. **7**, 174 (2025).

[6] S. F. Edwards and P. W. Anderson, Theory of spin glasses, J. Phys. F: Met. Phys. **5**, 965 (1975).

[7] D. Sherrington and S. Kirkpatrick, Solvable model of a spin-glass, Phys. Rev. Lett. **35**, 1792 (1975).

[8] M. Mézard, G. Parisi, and M. Virasoro, *Spin Glass Theory and Beyond*, World Scientific Lecture Notes in Physics, Vol. 9 (1986) p. 476, an Introduction to the Replica Method and Its Applications.

[9] H. Sompolinsky, N. Tishby, and H. S. Seung, Learning from examples in large neural networks, Phys. Rev. Lett. **65**, 1683 (1990).

[10] M. Opper and D. Haussler, Generalization performance

of Bayes optimal classification algorithm for learning a perceptron, Phys. Rev. Lett. **66**, 2677 (1991).
[11] H. S. Seung, H. Sompolinsky, and N. Tishby, Statistical mechanics of learning from examples, Phys. Rev. A **45**, 6056 (1992).
[12] T. L. H. Watkin, A. Rau, and M. Biehl, The statistical mechanics of learning a rule, Rev. Mod. Phys. **65**, 499 (1993).
[13] H. Nishimori, *Statistical Physics of Spin Glasses and Information Processing: An Introduction* (2001).
[14] C. Holzhey, F. Larsen, and F. Wilczek, Geometric and renormalized entropy in conformal field theory, Nucl. Phys. B **424**, 443 (1994).
[15] P. Calabrese and J. Cardy, Entanglement entropy and quantum field theory, J. Stat. Mech. **2004**, P06002 (2004).
[16] A. C. Barato and U. Seifert, Thermodynamic uncertainty relation for biomolecular processes, Phys. Rev. Lett. **114**, 158101 (2015).
[17] T. R. Gingrich, J. M. Horowitz, N. Perunov, and J. L. England, Dissipation bounds all steady-state current fluctuations, Phys. Rev. Lett. **116**, 120601 (2016).
[18] J. P. Garrahan, Simple bounds on fluctuations and uncertainty relations for first-passage times of counting observables, Phys. Rev. E **95**, 032134 (2017).
[19] A. Dechant and S.-i. Sasa, Current fluctuations and transport efficiency for general Langevin systems, J. Stat. Mech: Theory Exp. **2018**, 063209 (2018).
[20] I. Di Terlizzi and M. Baiesi, Kinetic uncertainty relation, J. Phys. A: Math. Theor. **52**, 02LT03 (2019).
[21] Y. Hasegawa and T. Van Vu, Uncertainty relations in stochastic processes: An information inequality approach, Phys. Rev. E **99**, 062126 (2019).
[22] Y. Hasegawa and T. Van Vu, Fluctuation theorem uncertainty relation, Phys. Rev. Lett. **123**, 110602 (2019).
[23] A. Dechant and S.-i. Sasa, Fluctuation–response inequality out of equilibrium, Proc. Natl. Acad. Sci. U.S.A. **117**, 6430 (2020).
[24] V. T. Vo, T. Van Vu, and Y. Hasegawa, Unified approach to classical speed limit and thermodynamic uncertainty relation, Phys. Rev. E **102**, 062132 (2020).
[25] T. Koyuk and U. Seifert, Thermodynamic uncertainty relation for time-dependent driving, Phys. Rev. Lett. **125**, 260604 (2020).
[26] P. Erker, M. T. Mitchison, R. Silva, M. P. Woods, N. Brunner, and M. Huber, Autonomous quantum clocks: Does thermodynamics limit our ability to measure time?, Phys. Rev. X **7**, 031022 (2017).
[27] K. Brandner, T. Hanazato, and K. Saito, Thermodynamic bounds on precision in ballistic multiterminal transport, Phys. Rev. Lett. **120**, 090601 (2018).
[28] F. Carollo, R. L. Jack, and J. P. Garrahan, Unraveling the large deviation statistics of Markovian open quantum systems, Phys. Rev. Lett. **122**, 130605 (2019).
[29] J. Liu and D. Segal, Thermodynamic uncertainty relation in quantum thermoelectric junctions, Phys. Rev. E **99**, 062141 (2019).
[30] G. Guarnieri, G. T. Landi, S. R. Clark, and J. Goold, Thermodynamics of precision in quantum nonequilibrium steady states, Phys. Rev. Research **1**, 033021 (2019).
[31] S. Saryal, H. M. Friedman, D. Segal, and B. K. Agarwalla, Thermodynamic uncertainty relation in thermal transport, Phys. Rev. E **100**, 042101 (2019).
[32] Y. Hasegawa, Quantum thermodynamic uncertainty relation for continuous measurement, Phys. Rev. Lett. **125**, 050601 (2020).
[33] Y. Hasegawa, Thermodynamic uncertainty relation for general open quantum systems, Phys. Rev. Lett. **126**, 010602 (2021).
[34] M. F. Sacchi, Thermodynamic uncertainty relations for bosonic Otto engines, Phys. Rev. E **103**, 012111 (2021).
[35] A. A. S. Kalaee, A. Wacker, and P. P. Potts, Violating the thermodynamic uncertainty relation in the three-level maser, Phys. Rev. E **104**, L012103 (2021).
[36] T. Van Vu and K. Saito, Thermodynamics of precision in Markovian open quantum dynamics, Phys. Rev. Lett. **128**, 140602 (2022).
[37] S. V. Moreira, M. Radaelli, A. Candeloro, F. C. Binder, and M. T. Mitchison, Precision bounds for multiple currents in open quantum systems, Phys. Rev. E **111**, 064107 (2025).
[38] K. Prech, P. P. Potts, and G. T. Landi, Role of quantum coherence in kinetic uncertainty relations, Phys. Rev. Lett. **134**, 020401 (2025).
[39] N. Ishida and Y. Hasegawa, Quantum computer-based verification of quantum thermodynamic uncertainty relation, arXiv:2402.19293 (2024).
[40] S. B. Nicholson, L. P. Garcia-Pintos, A. del Campo, and J. R. Green, Time-information uncertainty relations in thermodynamics, Nat. Phys. **16**, 1211 (2020).
[41] L. P. García-Pintos, S. B. Nicholson, J. R. Green, A. del Campo, and A. V. Gorshkov, Unifying quantum and classical speed limits on observables, Phys. Rev. X **12**, 011038 (2022).
[42] G. Biroli and J. P. Garrahan, Perspective: The glass transition, J. Chem. Phys. **138**, 12A301 (2013).
[43] N. Shiraishi, K. Funo, and K. Saito, Speed limit for classical stochastic processes, Phys. Rev. Lett. **121**, 070601 (2018).
[44] Y. Hasegawa, Unifying speed limit, thermodynamic uncertainty relation and Heisenberg principle via bulk-boundary correspondence, Nat. Commun. **14**, 2828 (2023).
[45] Y. Hasegawa and T. Nishiyama, Thermodynamic concentration inequalities and trade-off relations, Phys. Rev. Lett. **133**, 247101 (2024).
[46] L. Lovász, Random walks on graphs: A survey, in *Combinatorics, Paul Erdős is Eighty*, Vol. 2 (1996) pp. 353–398.
[47] J. D. Noh and H. Rieger, Random walks on complex networks, Phys. Rev. Lett. **92**, 118701 (2004).
[48] N. Masuda, M. A. Porter, and R. Lambiotte, Random walks and diffusion on networks, Phys. Rep. **716-717**, 1 (2017).
[49] S. Brin and L. Page, The anatomy of a large-scale hypertextual web search engine, Comput. Netw. ISDN Syst. **30**, 107 (1998).
[50] P. Pons and M. Latapy, Computing communities in large networks using random walks, in *Computer and Information Sciences – ISCIS 2005*, edited by pInar Yolum, T. Güngör, F. Gürgen, and C. Özturan (Berlin, Heidelberg, 2005) pp. 284–293.
[51] B. Perozzi, R. Al-Rfou, and S. Skiena, Deepwalk: online learning of social representations, in *Proc. 20th ACM SIGKDD Int. Conf. Knowl. Discov. Data Min.*, KDD '14 (New York, NY, USA, 2014) pp. 701–710.
[52] S. Köhler, S. Bauer, D. Horn, and P. N. Robinson, Walking the interactome for prioritization of candidate disease

genes, Am. J. Hum. Genet. **82**, 949 (2008).

[53] B. A. N. Travencólo and L. da F. Costa, Accessibility in complex networks, Phys. Lett. A **373**, 89 (2008).

[54] M. P. Viana, J. L. B. Batista, and L. d. F. Costa, Effective number of accessed nodes in complex networks, Phys. Rev. E **85**, 036105 (2012).

[55] J. Gómez-Gardeñes and V. Latora, Entropy rate of diffusion processes on complex networks, Phys. Rev. E **78**, 065102 (2008).

[56] Y. Hasegawa and T. Nishiyama, Thermodynamic entropic uncertainty relation, Phys. Rev. E **112**, 054140 (2025).

[57] G. T. Landi, M. J. Kewming, M. T. Mitchison, and P. P. Potts, Current fluctuations in open quantum systems: Bridging the gap between quantum continuous measurements and full counting statistics, PRX Quantum **5**, 020201 (2024).

[58] S. Nakajima and Y. Utsumi, Symmetric-logarithmic-derivative Fisher information for kinetic uncertainty relations, Phys. Rev. E **108**, 054136 (2023).

[59] T. Nishiyama and Y. Hasegawa, Exact solution to quantum dynamical activity, Phys. Rev. E **109**, 044114 (2024).

[60] T. Nishiyama and Y. Hasegawa, Tradeoff relations in open quantum dynamics via Robertson, Maccone-Pati, and Robertson-Schrödinger uncertainty relations, J. Phys. A: Math. Theor. **57**, 415301 (2024).

[61] U. Seifert, Stochastic thermodynamics, fluctuation theorems and molecular machines, Rep. Prog. Phys. **75**, 126001 (2012).

[62] V. V. Petrov, On lower bounds for tail probabilities, J. Stat. Plann. Inference **137**, 2703 (2007).

[63] H. Yunoki and Y. Hasegawa, Quantum speed limit and quantum thermodynamic uncertainty relation under feedback control, arXiv:2502.09081 (2025).